DEVELOPMENT OF POLYSILICON IGNITERS AND TEMPERATURE SENSORS FOR A MICRO GAS TURBINE ENGINE

X. Zhang, A. Mehra[†], A. A. Ayon[‡], and I. A. Waitz[†]

Department of Manufacturing Engineering and Fraunhofer USA Center for Manufacturing Innovation,
Boston University, Boston, MA 02215, USA
[†]Gas Turbine Laboratory, Massachusetts Institute of Technology, Cambridge, MA 02139, USA
[‡]Sony Semiconductor, 1 Sony Place, San Antonio, TX 78245, USA

ABSTRACT

This paper presents the development of microfabricated "on-chip" polysilicon igniters and temperature sensors for the combustion system of a micro gas turbine engine. We have reported the design and fabrication results of a novel through-wafer interconnect scheme that could greatly facilitate electrical contacts in multi-level MEMS devices by allowing direct electrical access to the backside of a wafer. This paper presents the results of a further effort that uses these interconnects to make electrical contacts to a thin-film polysilicon resistor so as to evaluate its ignition capability and its use as a wall temperature sensor for the micro gas turbine engine. An application of the through-wafer interconnects to a concept demonstration of thin-film polysilicon resistive igniters for the microengine showed that it was possible to initiate combustion and locally raise the temperature of the igniter to 900°C so long as the chip is thermally isolated. The results were found to be in good agreement with the predictions of an FEM thermal model. The possibility of using the resistors as temperature sensors is also examined. The non-linear variation of polysilicon resistivity with annealing temperatures due to complex effects resulting from dopant atom segregation, secondary grain growth and crystallographic relaxation reduced the operating range of the sensors to 450°C.

INTRODUCTION

As part of an initiative to develop a new generation of silicon power-MEMS, an effort is currently underway to produce 10-50 Watts of electrical power in a package that is less than one cubic centimeter in volume. The baseline design, applications and operation of such a device is presented by Epstein *et al.* [1]; the various turbomachinery, rotor-dynamic, electrical and combustion components are described in references [2-5].

Since such an engine will require electrical connections to the diagnostic elements and electrical components, it is necessary to develop a reliable electrical interconnect scheme. We have reported the design, fabrication, and experimental demonstration of through-wafer interconnects capable of allowing direct electrical access to the interior of a multilevel microelectromechanical system device [6]. The interconnects exploit the ability to conformally coat a high aspect ratio trench with a thick layer of tetraethylorthosilicate (TEOS) to isolate a through-wafer silicon plug that can provide electrical contact across two sides of a low resistivity wafer.

The difficulty in instrumenting micro-scale devices with conventional diagnostics also motivates the need for *in situ* sensors that are routinely microfabricated onto the chip as part of the fabrication process. In addition, since the final packaged device is intended to be a self-contained unit that is capable of independent operation, it will also require on-chip igniters to initiate combustion and start the heat engine.

This paper presents a concept demonstration of through-wafer interconnect application to thin-film polysilicon igniters and temperature sensors, and examines their behavior under high temperature operating conditions.

CONCEPT AND FABRICATION

As described earlier, the difficulty in taking out sealed wafer-level leads through bondlines motivated the development of a through-wafer interconnect scheme to allow direct electrical contact to the backside of the wafer. Conceived by Schmidt [6] and illustrated in Figure 1, the use of this novel technique can be expected to facilitate electrical connections in other microfabricated devices as well. The concept of this through-wafer interconnect exploits the ability to conformally coat a high-aspect ratio trench with a thick insulating layer so as to isolate a through-wafer via that can be used to provide electrical contact across two sides of a low-resistivity wafer. A fabrication demonstration and application of these interconnects to make electrical contacts to a second build of igniters and temperature sensors for the microengine has been reported elsewhere [6].

Using deep reactive ion etching (DRIE), 100 µm deep circular trenches were etched into the top surface of 300 µm n-type <100> silicon wafers that had a resistivity of 0.01-0.02 Ω cm. A 10 µm coating of TEOS was then deposited at 350°C in order to isolate the silicon plug from the rest of the substrate. Following the TEOS deposition, the oxide was
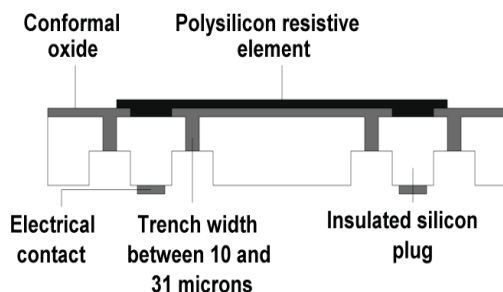

Figure 1: *Schematic of a through-wafer interconnect.*

chemically-mechanically polished down to the silicon surface to allow subsequent photolithography steps. 2 μm of TEOS was then additionally re-deposited and patterned to provide electrical access for the polysilicon. 0.5 μm thick polysilicon was then deposited at 625°C, POCl₃ phosphorus-doped at 925°C, and patterned to define the resistors. The resistor linewidth was 20 μm; the length was 2 mm. The design sheet resistivity was 10 Ω/square; the overall design resistance was approximately 5 kΩ. Finally, 100 μm wide circular trenches were dry-etched from the backside to release the isolated silicon plugs and provide electrical contact across the two sides of the wafer.

IGNITER DEVELOPMENT

Isolated igniter tests were conducted by using probe-tips to apply a voltage across the backside of the interconnect-pairs. Figure 2 shows the resistance and applied power as a function of the igniter temperature. The igniter temperature was measured with an IR camera calibrated to a polysilicon emissivity of 0.5. The figure shows increasing resistance and temperature with input power. The igniter current is of the order of tens of milliamperes, and corresponds to the intended current density of 10^5 A/cm². Figure 2 also shows that the power utilization of the igniters is between 3 and 6 Watts. In addition to depicting ohmic behavior over most of the operating range, the igniters were also observed to exhibit localized heating. Finally, Figure 2 shows experimental results for multiple runs, and for multiple dies, and indicates good repeatability of the results.

The igniters exhibited localized heating upon passage of current; Figure 3 shows one IR and one optical image showing the localized nature of this heating. The ignition capability of the igniters was also confirmed by passing a combustible hydrogen-air mixture over a single heater element (as shown in Figure 3). The igniter was able to reach a temperature of ~900°C and repeatedly ignite the mixture while consuming approximately 5 Watts of power.

To confirm this hypothesis, a finite-element heat transfer model was subsequently developed. Figure 4 plots the igniter surface temperature as a function of the input power and compares it with the experimental IR measurements. The numerical results agree with the experimental measurements to within 55°C, and suggest that the simplified resistor and interconnect geometry is sufficient to capture the temperature behavior of the igniter. Figure 4 also plots the amount of heat being conducted into the substrate, and shows that most of the input power is being dissipated via the silicon.

TEMPERATURE SENSOR DEVELOPMENT

This section discusses the use of the polysilicon resistors as temperature sensors for the engine. Use of the resistor as a temperature sensor is based on the ability to calibrate its resistance as a function of temperature, and then use an *in situ* measurement of the resistance to determine its temperature during operation. Figure 2(b) shows a
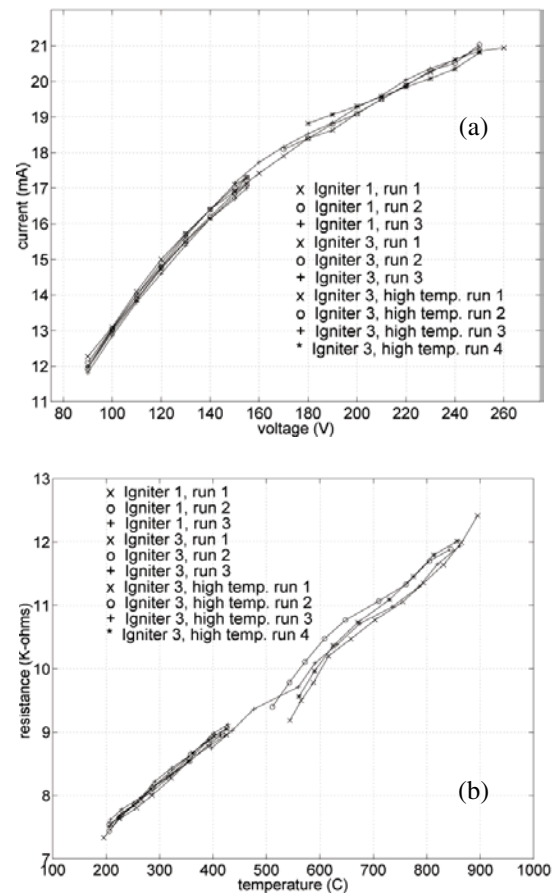

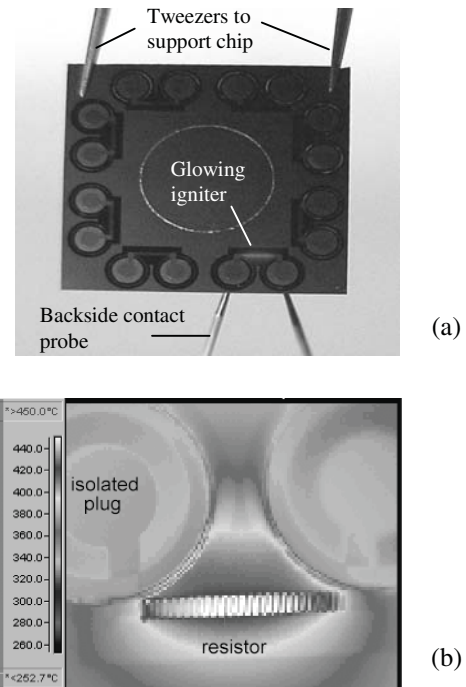**Figure 2:** *R versus T curves for multiple igniter runs showing good repeatability of the results.*

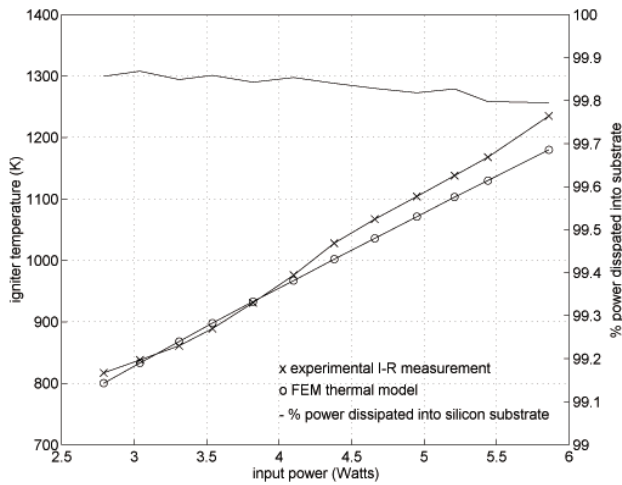**Figure 3:** *Optical and IR images of an igniter showing localized heating.*

Figure 4: *Numerically predicted values of the igniter surface temperature, showing good comparison with the experimental data.*

calibration curve obtained from the resistance versus temperature data for various igniter runs. The temperature-resistance relationship for the sensor was obtained by linearly fitting the data in Figure 2(b), and is given by: $R\ (k\Omega) = 6.1389 - 0.0068T\ (°C)$.

To test this capability, the resistors were exposed to a combustion environment with equivalence ratios between 0.3 and 0.7. The resistance-based sensor measurements were then compared with independent measurements from an adjacent thermocouple. The results show that the resistance-based measurements from the sensor differ by as much as 150°C from the thermocouple results. The difference in the two temperature measurements may be attributed to inaccuracies in the sensor calibration curve, however, more interestingly, it also shows a consistent increase in the sensor measurements with increasing exposure to hot combustion gases. Consequently, in order to understand the increase in film resistance, and to identify a stable operating range for the sensor, patterned polysilicon films on thermal oxide were subjected to three different annealing experiments.
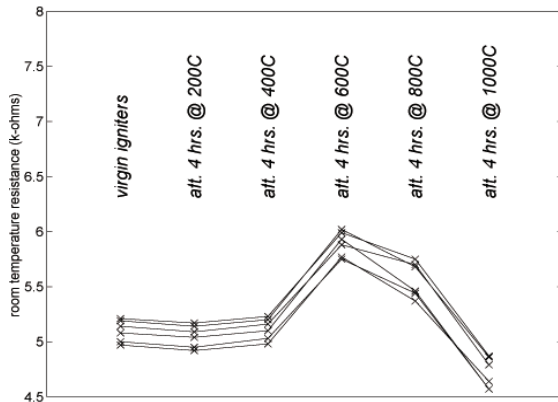

Figure 5: *Measurement of room temperature resistance of polysilicon igniters after progressive high temperature exposure.*

In experiment one, samples were progressively exposed to temperatures between 200°C and 1000°C for four hours. The room temperature resistance of the igniter was measured after each run, and as shown in Figure 5, remained stable until 400°C and then became non-linear after a 600°C thermal anneal. The initial increase in resistance may be explained by changes in the concentration of electrically active dopant atoms. Phosphorus atoms are known to diffuse towards the grain boundaries and become electrically inactive [7-10]. This phenomenon is known as dopant atom segregation, and can increase polysilicon resistance due to a reduction in the concentration of active carriers. At higher temperatures, the increase in resistance due to dopant atom segregation is countered by the combined and dominating influence of two additional phenomenon. First, secondary grain growth with increasing temperatures [7,9,11] increases carrier mobility due to a decrease in grain boundary scattering [12]. Second, crystallographic relaxation proposed by Colinge *et al.* partly removes grain boundary defects and increases the free carrier concentration at high temperatures [7]. At higher temperatures, effects due to crystallographic relaxation and secondary grain growth begin to dominate, causing the resistance to decrease from thereon.
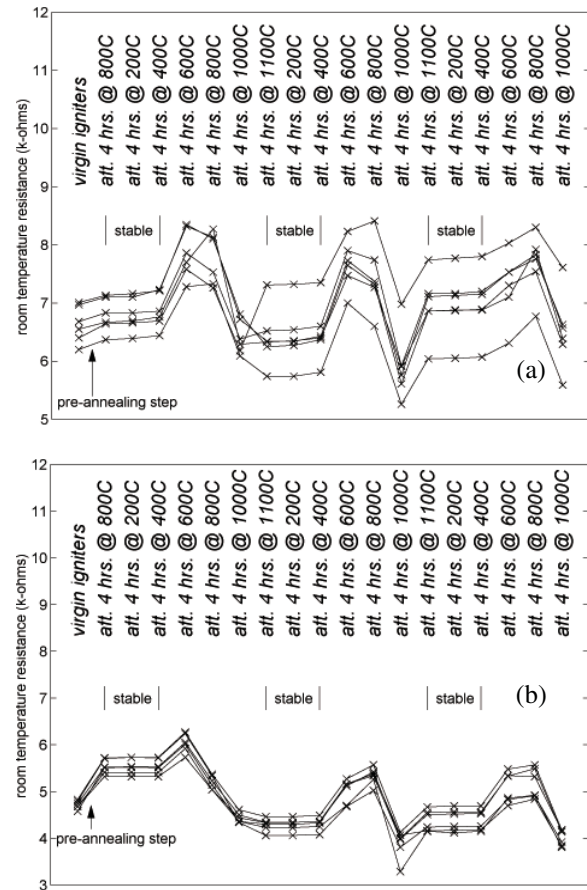

Figure 6: *Room temperature resistance measurements of a pre-annealed polysilicon resistor after progressive exposures to an inert high temperature environment. (a) Poly + TEOS sample, (b) Poly + thermal oxide sample.*
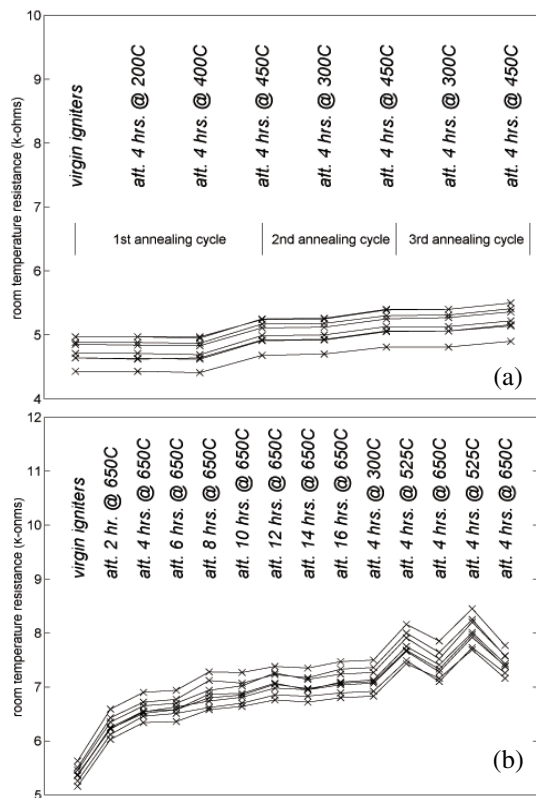
Figure 7: *Stability of the polysilicon resistance during repeated anneals up to 450°C and 650°C. (a) Stable resistance up to 450°C, (b) Changed resistance after an initial annealing-to-equilibrium step at 650°C.*

Experiment two was intended to see whether the sensor could be operated stably after an initial high temperature exposure of the type shown in Figure 5, and to evaluate the effects of multiple annealing cycles. The results are plotted in Figure 6, and show that the room temperature resistance of polysilicon following isochronal anneals settles into a cyclic pattern. Consistent with the observations of Makino *et al.* [11], this suggests that the resistance is predominantly determined by a combination of the solid solubility limit and the carrier mobility at each annealing temperature, and is therefore uniquely and reversibly determined by the last annealing temperature.

Experiment three was intended to determine a stable operating regime for the sensor. The results plotted in Figures. 5 & 6 suggest that the resistance of the polysilicon is stable for several tens of hours as long as it is annealed below 600°C. Additional tests actually showed that the resistance was barely stable up to 450°C (Figure 7 (a)). In order to stabilize the carrier concentration, the samples were sequentially annealed in an inert ambient at 650°C until the resistance was observed to reach the equilibrium value; the results are plotted in Figure 7 (b). It is seen that even after the sensor has been pre-annealed to equilibrium at 650°C, its resistance continues to reversibly change between equilibrium values at 525°C and 650°C, and is uniquely determined by the last annealing temperature in the 400°C-650°C range.

CONCLUSIONS

This paper described the development of microfabricated "on-chip" igniters and temperature sensors for the combustion system of the engine. The application of thin-film polysilicon resistive elements as igniters for the microengine combustor showed that it was possible to locally heat an isolated element up to 900°C and ignite a combustible hydrogen-air mixture. Prior to their integration into the microcombustor however, additional design changes are still needed to better insulate them from the supporting silicon substrate. The use of heavily doped polysilicon resistors as temperature sensors for the engine was also evaluated. The results suggested that a suitably calibrated sensor may be used in some of the cooler sections of the microengine up to temperatures of 400°C. This range is primarily limited by complex resistivity changes due to charge segregation, secondary grain growth and crystallographic relaxation effects that rendered the sensor difficult to calibrate.

REFERENCES

1. A. Epstein *et al.*, presented at 28th AIAA Fluid Dynamics and 4th AIAA Shear Flow Control Conference, Snowmass Village, June 1997.
2. S. Jacobson, presented at 29th AIAA Fluid Dynamics Conference, Albuquerque, 1998.
3. L. Frechette *et al.*, Technical Digest of Solid-State Sensors and Actuators Workshop, Hilton Head Island, SC, June 4-9, 2000, pp. 43-47.
4. A. Mehra *et al.*, Journal of Microelectromechanical Systems, Vol. 8, No. 2, pp. 152-160, June 1999.
5. A. Mehra *et al.*, Journal of Microelectromechanical Systems, Vol. 9, No. 4, pp. 517-527, December 2000.
6. A. Mehra *et al.*, Journal of Vacuum Science & Technology B, Vol. 18, No. 5, pp. 2583-2589, September/October 2000.
7. J. Colinge *et al.*, J. Electrochem. Soc.: Solid-State Science & Technology, Vol. 128, No. 9, pp. 2009-2014, September 1981.
8. E. Loh *et al.*, Journal of Applied Physics, Vol. 54, No. 8, pp. 4463-4466, August 1983.
9. Lu *et al.*, IEEE Trans. on Electron Devices, Vol. ED-30, pp.137, 1983.
10. J. Murota *et al.*, Journal of Applied Physics, Vol. 53, No. 5, pp. 3702-3708, May 1982.
11. T. Makino *et al.*, Solid-State Electronics, Vol. 24, pp. 49-55, 1981.
12. S. Solmi *et al.*, J. Electrochem. Soc.: Solid-State Science & Technology, Vol. 129, No. 8, pp. 1811-1818, August 1982.